



## 12 **Abstract**

13 In India, biomedical waste (BMW) management is governed by strict regulations to mitigate health  
14 and environmental risks. It includes materials such as sharps, infectious wastes, pharmaceuticals,  
15 and non-hazardous items contaminated with potentially infectious substances. Proper management  
16 and disposal of BMW are critical to prevent environmental contamination and health risks. This  
17 article introduces an Enhanced U-Net (EnU-Net) integrated with Deep Neural Network  
18 BMW Classification (EnU-Net-DNN-BMWC) to enhance accuracy in this critical task.  
19 Leveraging the U-Net framework with an Encoder-Decoder Network (EDN) and pixel-wise  
20 classification layer initially optimizes image segmentation. Bayesian functions mitigate  
21 segmentation uncertainties, while Content-Sensitive Sampling (CSS) refines pixel sampling to  
22 prioritize data-sparse regions. Data collected from G. Kuppuswamy Naidu Memorial Hospital and  
23 Kovai Medical Center and Hospital (KMCH) in Coimbatore over six months, categorizing sharps,  
24 infectious materials, pharmaceuticals, and non-hazardous waste, informs waste management  
25 strategies. Experimental validation using 100 biomedical waste images demonstrates EnU-Net-  
26 DNN-BMWC achieving good accuracy, surpassing standalone DNN-BMWC using Matlab 2022.  
27 The comparative analysis across different metrics such as accuracy, precision, F-measure, recall,  
28 error rate, and RMSE between DNN-BMWC and the proposed EnU-Net-DNN-BMWC  
29 framework were evaluated in this study, highlighting EnU-Net-DNN-BMWC's superior  
30 performance. Finally, this study underscores EnU-Net-DNN-BMWC's efficacy in enhancing  
31 biomedical waste classification, crucial for sustainable waste management practices and regulatory  
32 compliance in healthcare settings.

33 **Keywords:** *Biomedical waste, deep learning, U-Net, encoder, decoder, Deep Neural Network*

## 34 **1. Introduction**

35 The management and disposal of biomedical waste (BMW), a consequence of healthcare  
36 operations, presents substantial issues. It includes a wide range of substances, including medicines,  
37 contaminated materials, sharps, and medical trash. Minimizing health risks and environmental  
38 damage requires proper characterization and management of BMW. Precise division and  
39 categorization of these waste products are necessary for their proper removal and handling,  
40 ensuring that dangerous elements are managed appropriately and cutting down on total waste  
41 management expenses. The manual sorting and categorization method used in biomedical waste  
42 management is labor-intensive and frequently inconsistent. Automated systems that use machine  
43 learning and computer vision techniques have been presented as solutions to these problems. These  
44 technologies use sophisticated image processing and classification techniques to improve BMW  
45 management's accuracy and efficiency.

46 The Enhanced U-Net (EnU-Net) is specifically designed for precise image segmentation,  
47 making it ideal for identifying various biomedical waste types in complex images. Its encoder-  
48 decoder structure captures both global and local features, ensuring accurate delineation of waste  
49 items. The Deep Neural Network (DNN) complements this by effectively classifying the  
50 segmented outputs based on learned patterns. By integrating these two architectures within the  
51 EnU-Net-DNN-BMWC framework, we capitalize on U-Net's segmentation capabilities to provide  
52 detailed inputs for the DNN, thereby enhancing classification accuracy. This synergy results in a  
53 more robust and efficient system for biomedical waste management.

54 In this regard, an important advancement in this field is the suggested Enhanced Segmentation  
55 Network (EnU-Net), combined with a Deep Neural Network for Biomedical Waste Classification  
56 (EnU-Net-DNN-BMWC). Building on the U-Net architecture, a well-known model for medical  
57 picture segmentation, is the EnU-Net framework. Because U-Net is capable of fine-grained picture

58 segmentation, its architecture combines an Encoder-Decoder Network (EDN) with a pixel-wise  
59 classification layer. To extract hierarchical characteristics from the image, the encoder gradually  
60 reduced. Then, the decoder upsamples these features to restore the spatial resolution, enabling  
61 accurate pixel-level classification. The U-Net framework does have certain drawbacks, despite its  
62 effectiveness. The inherent ambiguity in segmentation resulting from different image qualities and  
63 various waste compositions is one prominent obstacle. In order to tackle this issue, the EnU-Net  
64 architecture incorporates uncertainty estimates through the integration of Bayesian functions,  
65 hence enabling more resilient pixel sampling and minimizing segmentation mistakes.

66 The application of Bayesian functions to mitigate segmentation uncertainties is indeed a valuable  
67 strategy. To enhance the manuscript, it would be beneficial to provide a comprehensive overview  
68 of the implementation process of these functions. This includes detailing how prior distributions  
69 are defined, how likelihoods are calculated from segmentation outputs, and how posterior  
70 distributions are derived to update model predictions.

71 Additionally, discussing the specific types of Bayesian methods used, such as Bayesian inference  
72 or Monte Carlo sampling, would clarify their roles in reducing uncertainty. It's also important to  
73 present quantitative results demonstrating the impact of these Bayesian functions on model  
74 performance, such as improvements in accuracy, precision, and recall. Including visual examples  
75 of segmentation outputs before and after applying Bayesian methods could further illustrate their  
76 effectiveness, thus enriching the overall understanding of their contribution to the model's  
77 robustness.

78

79 Moreover, Content-Sensitive Sampling (CSS) is implemented by the framework to improve  
80 segmentation precision in data-sparse regions. In locations with less information, CSS deliberately

81 gives detailed pixel sampling priority, while in denser areas, it conserves processing resources. By  
82 streamlining the segmentation procedure, this method guarantees a more accurate analysis of  
83 crucial areas. The potential of the EnU-Net-DNN-BMWC system to transform biomedical waste  
84 management procedures is highlighted by this study. It provides a promising way to raise the  
85 effectiveness and precision of BMW disposal and treatment procedures, which will ultimately lead  
86 to better environmental and public health results. It does this by fusing improved segmentation  
87 with sophisticated classification approaches.

88 Some recent kinds of literature provide valuable insights into different aspects of biomedical waste  
89 management, highlighting the role of technology and innovative approaches in addressing this  
90 critical issue. A range of artificial intelligence (AI) methods improve trash management  
91 procedures, including prediction models for waste generation and machine learning algorithms for  
92 waste classification. The focus of the article is on how AI can optimize resource allocation,  
93 enhance accuracy, lower human error, and update waste management procedures (Sarkar et al.,  
94 2023)

95 Using multivariate recurrent neural networks, a sophisticated method for anticipating the creation  
96 of biological waste during sanitary situations was provided by (Galvan-Alvarez et al. 2023). Their  
97 research highlights how improving waste management systems in urban environments requires  
98 precise forecasting models. This method ensures prompt intervention, reduces health hazards  
99 associated with inappropriate waste treatment, and improves readiness and resource allocation  
100 during emergencies. New technologies that support efficient BMW disposal and long-term  
101 management, especially in the context of the COVID-19 pandemic were investigated by (Kumbhar  
102 et al., 2024). They talk about a range of technologies that handle the spike in the creation of  
103 biological waste during the epidemic, including automated waste processing systems and

104 sophisticated sterilization techniques. In order to increase effectiveness and safety, this analysis  
105 emphasizes how crucial it is to incorporate new technology into the frameworks already in place  
106 for waste management. Research on the use of artificial intelligence (AI) in the management of  
107 biomedical waste has been extensive. (Sengeni et al. 2023) offer AI-based approaches for  
108 managing biological waste with an emphasis on improving safety and streamlining disposal  
109 procedures. Their work offers insights into how artificial intelligence (AI) might improve and  
110 automate waste sorting and processing, hence streamlining waste management methods. It is  
111 included in the Handbook of Research on Safe Disposal Methods of Municipal Solid Wastes.

112 By presenting forth an IoT-tracked, fuzzy classified integrated technique for biomedical waste  
113 management, (Wawale et al. 2022) also contribute to this field. Their method tracks and classifies  
114 waste in real time using fuzzy logic and Internet of Things (IoT) technologies, guaranteeing more  
115 precise and effective management. The environmental effects of dental clinics' biomedical waste  
116 management are discussed by (Subramanian et al. 2021). Their research raises important questions  
117 about how biomedical waste is disposed of in dental settings, emphasizing the need for improved  
118 procedures and adherence to laws in order to prevent environmental harm. The understanding of  
119 BMW's environmental impact is deepened by this collaboration, especially in specialized sectors  
120 like dentistry.

121 However, the prospects, difficulties, and current developments in the field of biomedical waste  
122 management (Kannadhasan and Nagarajan 2022). Their analysis offers a thorough summary of  
123 contemporary problems and developments, including the application of deep learning and machine  
124 learning methods to improve waste management procedures. The focus of this work is on how  
125 BMW management is changing and how technology might help solve long-standing problems.  
126 (Achuthan and Madan Gopal 2016) explain the accuracy and efficiency of waste segregation are

127 critical for efficient waste management, and this study offers a novel way to increase these metrics.  
128 To improve waste processing, the hybrid model combines the benefits of optimization and  
129 clustering methodologies.

130 Additionally, a fuzzy TOPSIS-based method for the thorough assessment of biological waste  
131 management. By adding fuzzy logic to the evaluation process, this approach promotes  
132 sustainability and decision-making by allowing for more accurate and nuanced analyses of waste  
133 management techniques (Al-Sulbi et al. 2023). Their efforts aid in the creation of stronger  
134 frameworks for assessing and enhancing BMW management systems. (Zulqarnain et al. 2024) use  
135 an interval-valued q-rung ortho-pair fuzzy soft set-based EDAS algorithm to evaluate different  
136 biomedical waste disposal methods. A thorough analysis of disposal strategies, stressing the  
137 advantages and disadvantages of various approaches in different situations. Their method offers  
138 insightful information on improving disposal procedures through quantitative evaluations (Gopi et  
139 al., 2020).

140 Biomedical waste management has been significantly impacted by the COVID-19 epidemic. The  
141 pandemic's effects on the buildup of biomedical waste are discussed by (Pavithiran et al. 2022),  
142 who also offer practical treatment solutions. Their research emphasizes how urgently strong waste  
143 management solutions are needed to address the pandemic's increased trash generation and related  
144 issues. The COVID-19 crisis's effects on waste management policy adherence and practices are  
145 reviewed by (Costa et al. 2023). Their narrative study clarifies how the pandemic has impacted  
146 waste management practices and regulations, offering a critical viewpoint on the necessity of more  
147 stringent management protocol adherence as well as adaptive methods.

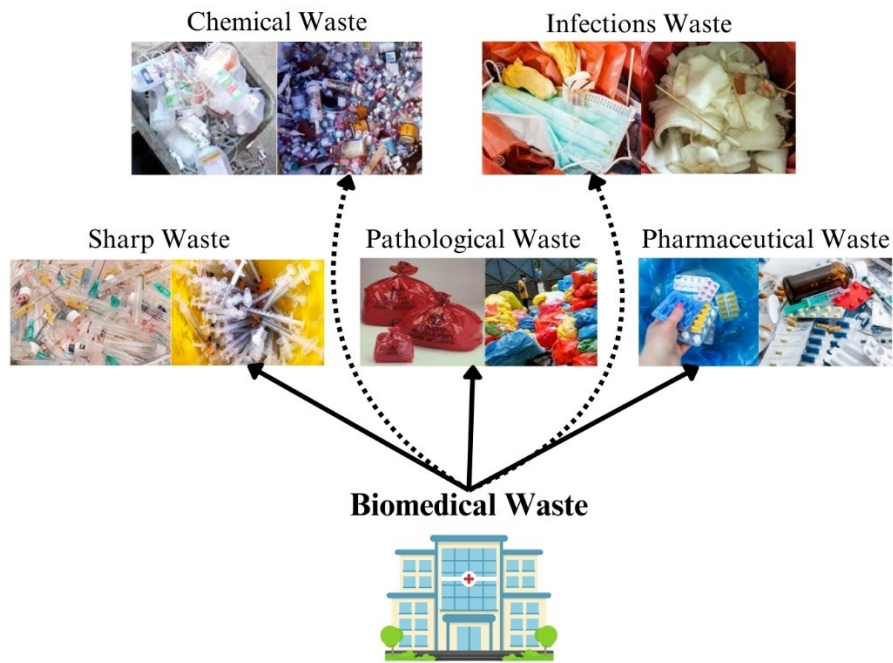
## 148 **2. Proposed Methodology**

### 149 *2.1. Data collection*

150 Data for biomedical waste was collected from two prominent hospitals in Coimbatore, namely G.  
151 Kuppuswamy Naidu Memorial Hospital and Kovai Medical Center and Hospital (KMCH). The  
152 study focused on analyzing waste types, quantities, and composition to develop a comprehensive  
153 understanding of waste management practices in healthcare settings. Collected over six months,  
154 the data included detailed categorization of biomedical waste such as sharps, infectious materials,  
155 pharmaceuticals, and non-hazardous waste. This information is crucial for optimizing disposal  
156 strategies and ensuring compliance with regulatory standards. The empirical data gathered from  
157 these hospitals forms the basis for assessing current practices and proposing efficient, sustainable  
158 solutions in biomedical waste management tailored to local conditions in Coimbatore.

## 159 *2.2. Dataset*

160 This research uses MATLAB 2022 to compare the EnU-Net-DNN-BMWC framework's  
161 performance against that of the DNN-TC framework. 200 images of various biomedical wastes  
162 are used to evaluate the frameworks. These images are divided into five categories: sharp waste  
163 (scalpels, blades, and needles), pharmaceutical waste (residual medications and spills), infectious  
164 waste (discarded gloves, masks, and blood-soaked bandages), and pathological waste (solids and  
165 surgical fluids). For training and testing, the dataset is divided into 100 photos each. Figure 1  
166 displays graphic depictions of example photos from the biomedical waste dataset.



167

168

**Figure 1:** Image dataset

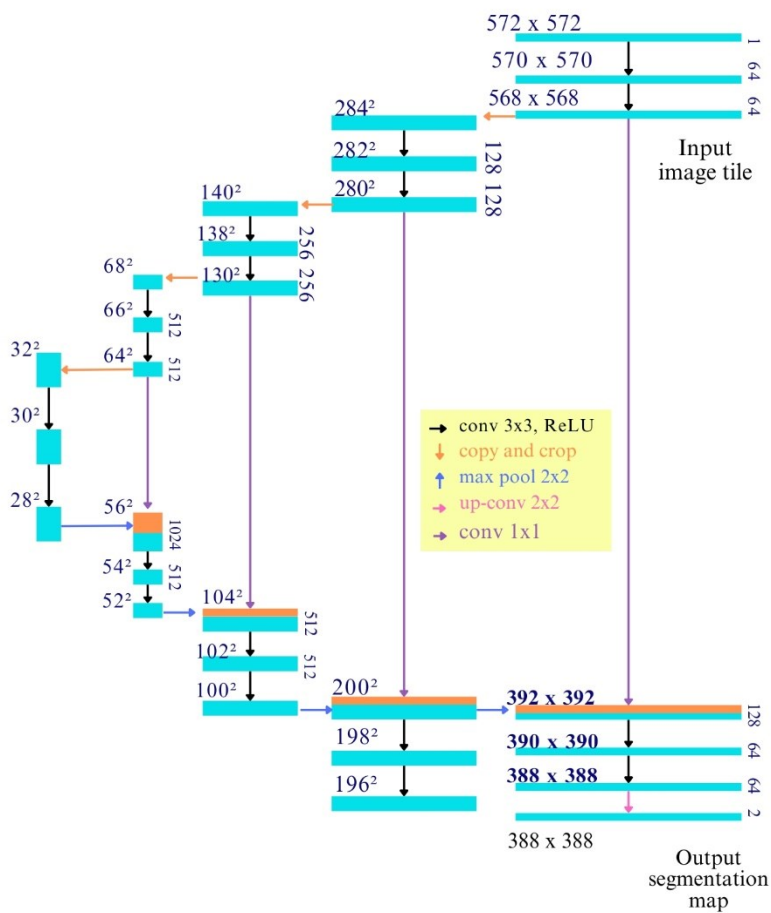
169 *2.3. Proposed method*

170 An extensive overview of the EnU-Net-DNN-TC framework is given in this section. This approach  
 171 uses the EDN as its primary training unit and is inspired by the ideas of unsupervised feature  
 172 learning. To create feature maps, the encoder phase combines pixel-wise tanh non-linearity, filter  
 173 convolution, subsampling, and max-pooling. The decoder receives these high-level feature maps  
 174 and uses aggregated learning variables to upsample them. Lastly, these upsampled maps are  
 175 convolved to reconstitute the original picture.

176 *2.4. Design of U-Net framework*

177 Convolutional network design, or u-net, allows for quick and accurate picture segmentation.  
 178 Strongly utilized for semantic segmentation tasks, especially in biological image analysis, is the  
 179 U-Net framework. Its exact pixel-level classification is made possible by its encoder-decoder

180 structure with skip connections, which is a design feature that has proved crucial to many medical  
 181 imaging applications. Skip connections, which establish direct links between corresponding levels  
 182 between the encoder and decoder, are one of U-Net's unique characteristics. These interfaces help  
 183 with accurate object localization during segmentation by transferring feature maps from the  
 184 encoder to the decoder. U-Net successfully preserves the fine-grained information required for  
 185 precise segmentation by fusing upsampled features from the decoder with high-resolution features  
 186 from the encoder. U-Net uses transposed convolutions, often referred to as deconvolutions, in the  
 187 decoder portion of the network to upsample the feature maps. Figure 2 demonstrates the  
 188 architecture of the U-Net.



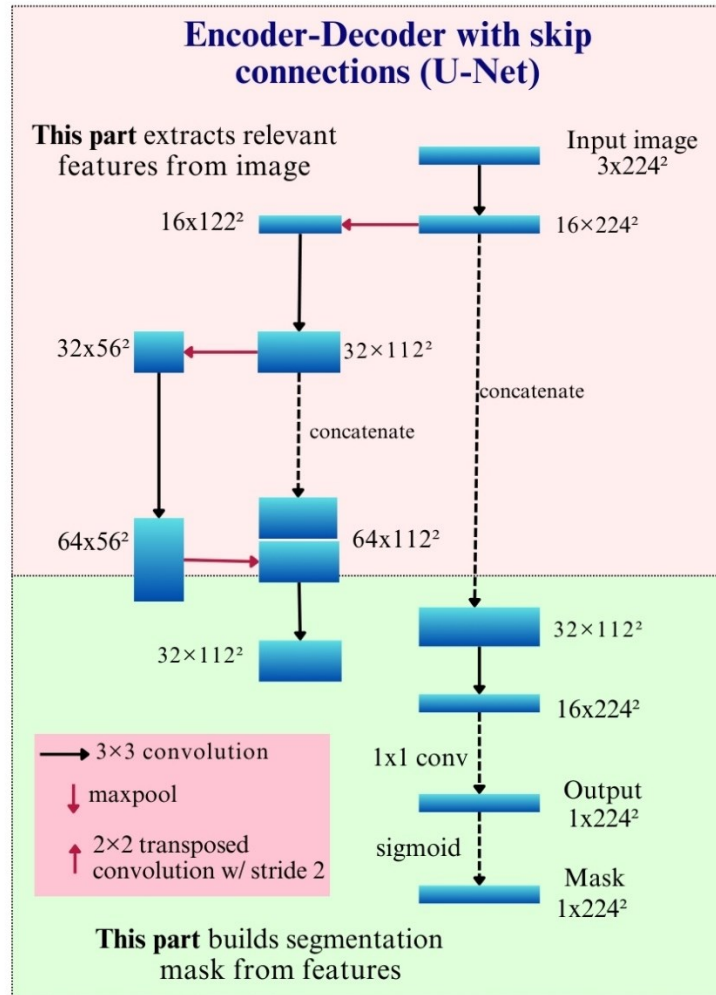
189

190

**Figure 2:** The architecture of the U-Net framework

191 This procedure intends to restore the spatial resolution that was lost during the encoder stage's  
192 downsampling. U-Net aligns with the original input size by gradually upsampling to recreate the  
193 segmented image with pixel-level accuracy. A pixel-wise classification layer, or softmax layer in  
194 the case of multi-class segmentation problems, is the last layer in the U-Net architecture. This layer  
195 divides the image into discrete areas according to learned features by assigning a probability  
196 distribution to every pixel within the specified classes. U-Net is renowned for its parameter  
197 efficiency, using fewer parameters than fully convolutional networks of comparable depth, yet  
198 having a deep architecture. Because of this feature, U-Net performs well on jobs requiring a lot of  
199 computational power or little training data, which is typical in medical imaging. Numerous  
200 biomedical imaging applications, including organ localization, tumor detection, and cell  
201 segmentation, have seen widespread application of U-Net. Researchers and practitioners in the  
202 healthcare field appreciate it because of its robust performance and ability to handle complex  
203 structures and different textures in medical images.

204 U-Net is essentially made up of two networks: an encoder network and a decoder network. The  
205 encoder employs convolutional and pooling layers to increase the depth of the input image while  
206 gradually decreasing its spatial dimensions, much like conventional convolutional neural networks  
207 (CNNs). High-level features are extracted from the input image through this technique, which  
208 captures both local and global context. The effectiveness of the U-Net framework in semantic  
209 segmentation tasks is demonstrated by its design, which makes use of an encoder-decoder  
210 architecture with skip connections and effective upsampling. This is especially important in  
211 biomedical imaging, where exact localization and accurate segmentation are critical. the design of  
212 the U- Net decoder is structured in Figure 3.



213

214

**Figure 3:** Design of UNet decoder

215 *2.5. Application of CSS to the suggested EnU-Net framework*

216 By using Content-Sensitive Sampling (CSS) to improve semantic segmentation, the EnU-Net  
 217 system solves the problem of efficiently sampling pixels with different data densities in biomedical  
 218 pictures. By dynamically modifying the sample rate in response to local image information, CSS  
 219 enhances pixel sampling and increases segmentation accuracy across various locations of interest.

220 With CSS, adaptive pixel sampling is made possible by integrating Bayesian uncertainty estimates  
 221 into the U-Net architecture. By prioritizing regions with limited data, CSS ensures that the model

222 focuses on underrepresented areas, enhancing its ability to learn from diverse examples. This  
 223 approach mitigates biases that can arise from over-represented classes and improves overall model  
 224 robustness. CSS works by analyzing content characteristics within the dataset to identify these  
 225 sparse regions, allowing for targeted sampling that enriches the training process. This strategic  
 226 emphasis not only optimizes the model's performance but also promotes a more balanced  
 227 representation of the data, leading to improved segmentation and classification accuracy in  
 228 complex scenarios. By incorporating CSS, the framework effectively enhances its learning  
 229 capabilities, ultimately contributing to more reliable and precise outcomes in biomedical waste  
 230 management. The goal of this methodological improvement is to save resources in less important  
 231 portions of the image while allocating computational power to areas of the image that need finer  
 232 segmentation information. The Bayesian Uncertainty Estimation equation (1-5) is as follows :

$$233 \quad \sigma_i^2 = \mathbb{E}[(y_i - \hat{y}_i)^2] \quad (1)$$

234 Here,  $\sigma_i^2$  represents the uncertainty associated with the pixel  $i$  in the segmentation output, where  
 235  $y_i$  is the ground truth and  $\hat{y}_i$  is the predicted segmentation label.

$$236 \quad p_i = \frac{1}{1 + \exp(-\alpha \cdot \sigma_i)} \quad (2)$$

237 The sampling probability  $p_i$  adjusts based on the estimated uncertainty  $\sigma_i$  using a sigmoid function  
 238 parameterized by  $\alpha$ . Higher uncertainty leads to higher sampling probability.

$$239 \quad \mathcal{L} = \mathcal{L}_{\text{seg}} + \lambda \sum_i p_i \cdot \mathcal{L}_{\text{aux}}(x_i, y_i) \quad (3)$$

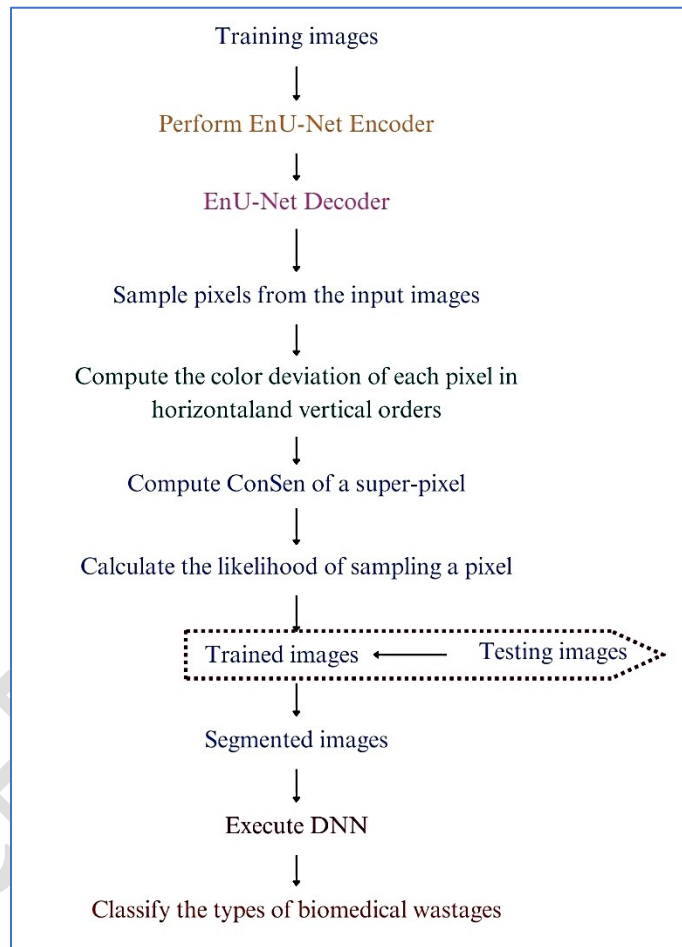
240 The total loss  $\mathcal{L}$  combines segmentation loss  $\mathcal{L}_{\text{seg}}$  and auxiliary loss  $\mathcal{L}_{\text{aux}}$  weighted by the sampling  
 241 probability  $p_i$  and a regularization parameter  $\lambda$ .

$$242 \quad \text{Sampling Rate} = \sum_i p_i \quad (4)$$

243 The sampling rate dynamically adjusts during training based on the computed sampling  
 244 probabilities  $p_i$  across all pixels.

245 
$$\theta_{\text{new}} = \theta_{\text{old}} - \eta \cdot \nabla_{\theta} \mathcal{L} \tag{5}$$

246 During optimization, where  $\theta$  represents  $t \downarrow$  model parameters, updates are performed using the  
 247 gradient  $\nabla_A \mathcal{L}$  with a learning rate  $n$ .



248

249 **Figure 4:** Flow diagram of EnU-Net-DNN-BMWC framework

250 By using Bayesian uncertainty estimates to dynamically modify pixel sampling rates during  
 251 training, CSS improves the EnU-Net architecture. Through the use of a sigmoid function, the  
 252 sampling probability  $p_i$  is influenced by the uncertainty  $\sigma_i$ , which represents the model's level of

253 confidence in each pixel prediction. Greater sampling probabilities are assigned to pixels with  
254 greater uncertainty, so resources are distributed more efficiently to areas where segmentation  
255 accuracy is critical. EnU-Net enhances segmentation accuracy across biological pictures by  
256 optimizing computing resources through the incorporation of CSS. By precisely identifying and  
257 classifying waste materials, this adaptive strategy not only improves model performance but also  
258 makes biomedical waste management more efficient.

---

### 259 **Proposed algorithm**

---

260 Input: Image set

261 Output: Classified biomedical wastage classes

262 Initialize;

263 for(each input image)

264 Perform the encoder of EnU-Net;

265 Execute the decoder of EnU-Net;

266 for(each pixel in image)

267 Calculate the color variation of each pixel;

268 Compute the likelihood of each pixel being sampled;

269 Sample pixels in the data-sparse regions;

270 end for

271 Train the EnU-Net in an end-to-end manner; obtain

272 the segmented images;

273 Apply DNN classifier;  
274 Find the category of biomedical wastage;  
275 end for  
276 End

---

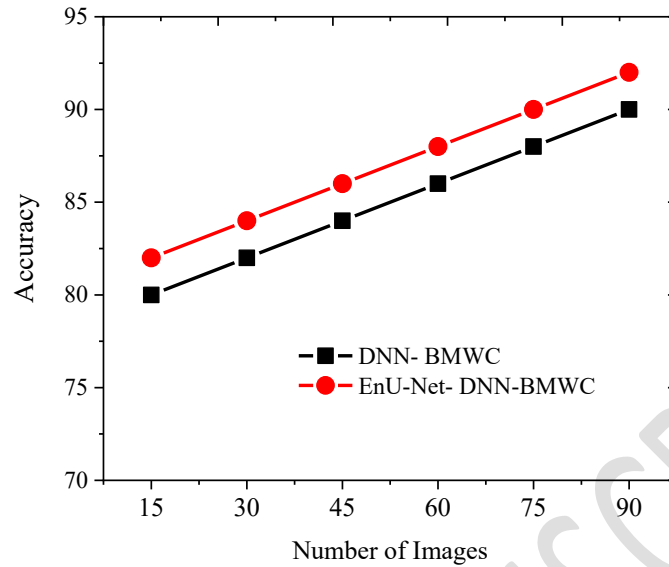
277

### 278 **3. Results**

279 In this section, the comparison is carried out based on precision, recall, f-measure, accuracy, error  
280 rate, and Root Mean Squared Error (RMSE).

#### 281 *3.1. Accuracy*

282 Figure 5 presents a comparative analysis of accuracy between DNN-BMWC and the proposed  
283 EnU-Net-DNN-BMWC across different numbers of images. The results show a consistent  
284 improvement in accuracy for EnU-Net-DNN-BMWC over DNN-BMWC at each increment of  
285 image count. Specifically, starting from 15 images, EnU-Net-DNN-BMWC achieves 82%  
286 accuracy compared to 80% for DNN-BMWC, and this trend continues with EnU-Net-DNN-  
287 BMWC consistently outperforming DNN-BMWC by 2% at each subsequent stage. By the time  
288 the dataset reaches 90 images, EnU-Net-DNN-BMWC achieves 92% accuracy, showcasing its  
289 superior performance in image classification tasks compared to the baseline DNN-BMWC model.

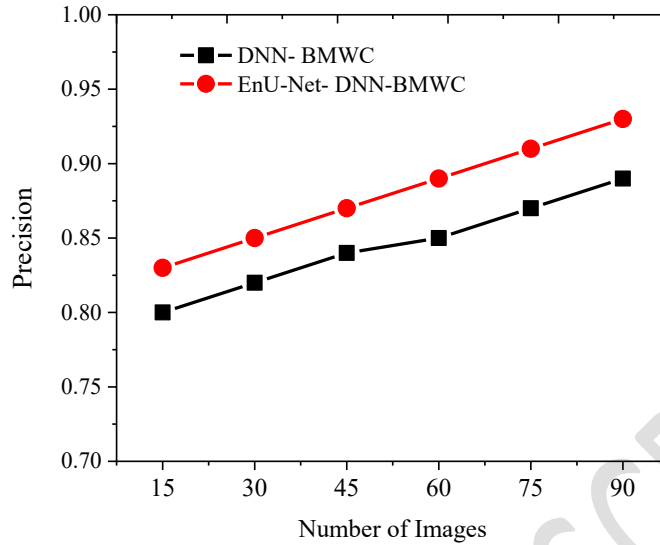


290

291 **Figure 5:** Comparison of DNN BMWC's Accuracy with the Proposed EnU-Net-DNN-BMWC

292 *3.2. Precision*

293 Figure 6 illustrates a comparative analysis of precision between DNN-BMWC and the proposed  
 294 EnU-Net-DNN-BMWC across varying numbers of images. The data shows a consistent  
 295 improvement in precision for EnU-Net-DNN-BMWC over DNN-BMWC as the number of images  
 296 increases. Starting with 15 images, EnU-Net-DNN-BMWC achieves a precision of 0.83, compared  
 297 to 0.8 for DNN-BMWC. This trend continues with EnU-Net-DNN-BMWC consistently  
 298 surpassing DNN-BMWC by 0.03 to 0.04 precision points at each subsequent stage. By the time  
 299 the dataset reaches 90 images, EnU-Net-DNN-BMWC achieves a precision of 0.93, demonstrating  
 300 its superior performance in precision-oriented tasks compared to the baseline DNN-BMWC  
 301 model.

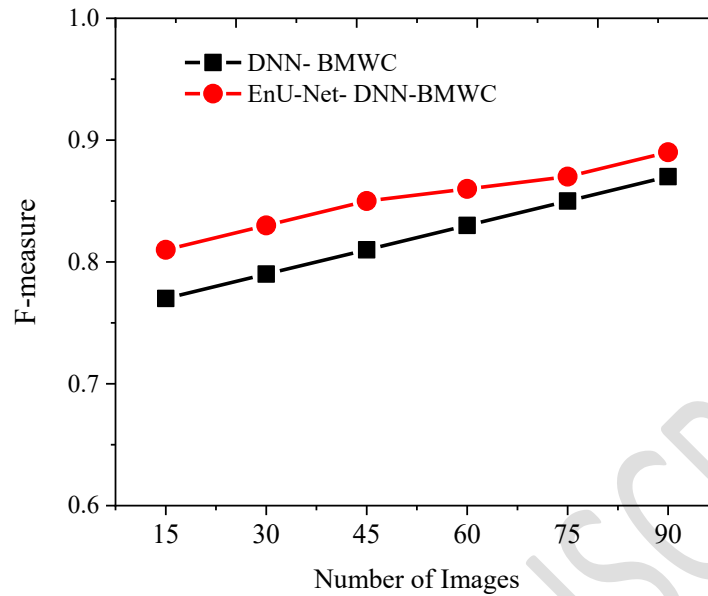


302

303 **Figure 6.** Precision Comparison of the proposed EnU-Net-DNN-BMWC and DNN BMWC

304 *3.3. F-measure*

305 Figure 7 depicts a comparative analysis of the F-measure between DNN-BMWC and the proposed  
 306 EnU-Net-DNN-BMWC across varying numbers of images. The results consistently show that  
 307 EnU-Net-DNN-BMWC outperforms DNN-BMWC in F-measure as the dataset size increases.  
 308 Beginning with 15 images, EnU-Net-DNN-BMWC achieves an F-measure of 0.81, compared to  
 309 0.77 for DNN-BMWC. This performance gap widens with each increment in the number of  
 310 images, with EnU-Net-DNN-BMWC consistently achieving higher F-measure scores than DNN-  
 311 BMWC. By the time the dataset includes 90 images, EnU-Net-DNN-BMWC achieves an F-  
 312 measure of 0.89, indicating its superior capability in achieving a balance between precision and  
 313 recall compared to the baseline DNN-BMWC model



314

315 **Figure 7:** Comparing the F-measures of the proposed EnU-Net-DNN-BMWC with the DNN

316 BMWC

317 *3.4. Recall*

318 Figure 8 presents a comparative analysis of recall between DNN-BMWC and the proposed EnU-

319 Net-DNN-BMWC across varying numbers of images. The results consistently demonstrate that

320 EnU-Net-DNN-BMWC achieves higher recall scores compared to DNN-BMWC as the dataset

321 size increases. Beginning with 15 images, EnU-Net-DNN-BMWC achieves a recall of 0.8, while

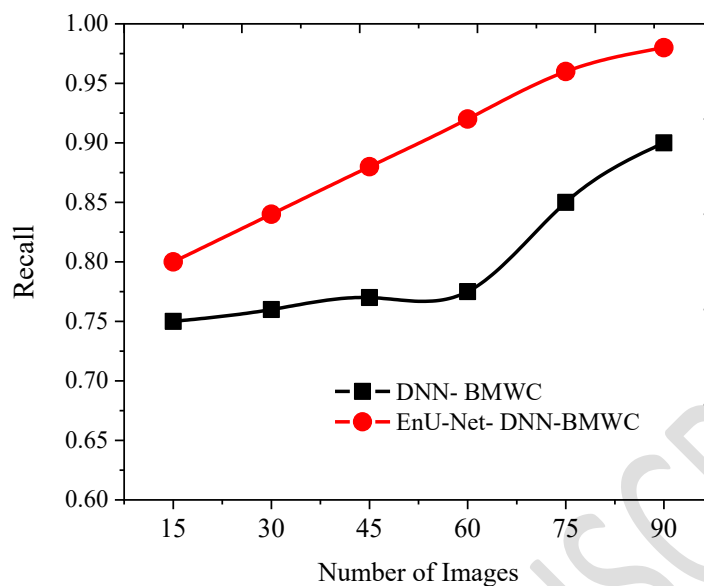
322 DNN-BMWC achieves 0.75. This performance gap continues to widen with each increment in the

323 number of images, with EnU-Net-DNN-BMWC consistently achieving superior recall scores. By

324 the time the dataset reaches 90 images, EnU-Net-DNN-BMWC achieves a recall of 0.98,

325 highlighting its enhanced ability to correctly identify relevant instances compared to the baseline

326 DNN-BMWC model

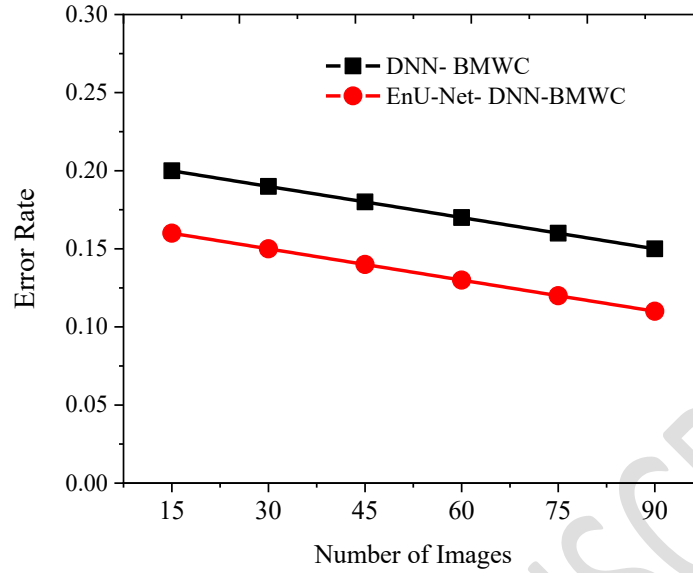


327

328 **Figure 8.** Comparing the proposed EnU-Net-DNN-BMWC with the recall of the DNN BMWC

329 *3.5. Error rate*

330 Figure 9 illustrates a comparative analysis of the error rate between DNN-BMWC and the  
 331 proposed EnU-Net-DNN-BMWC across different numbers of images. The data consistently shows  
 332 that EnU-Net-DNN-BMWC exhibits lower error rates compared to DNN-BMWC as the dataset  
 333 size increases. Starting with 15 images, EnU-Net-DNN-BMWC achieves an error rate of 0.16,  
 334 compared to 0.2 for DNN-BMWC. This trend continues with EnU-Net-DNN-BMWC consistently  
 335 reducing its error rate by 0.01 to 0.05 for each subsequent increment in the number of images. By  
 336 the time the dataset includes 90 images, EnU-Net-DNN-BMWC achieves an error rate of 0.11,  
 337 demonstrating its superior performance in minimizing classification errors compared to the  
 338 baseline DNN-BMWC model.



339

340 **Figure 9:** Error Rate Comparison between DNN BMWC and the Proposed EnU-Net-DNN-

341 BMWC

### 342 3.6. RMSE

343 Figure 10 compares the Root Mean Square Error (RMSE) between DNN-BMWC and the proposed

344 EnU-Net-DNN-BMWC across different numbers of images. The results consistently demonstrate

345 that EnU-Net-DNN-BMWC achieves lower RMSE values compared to DNN-BMWC as the

346 dataset size increases. Beginning with 15 images, EnU-Net-DNN-BMWC achieves an RMSE of

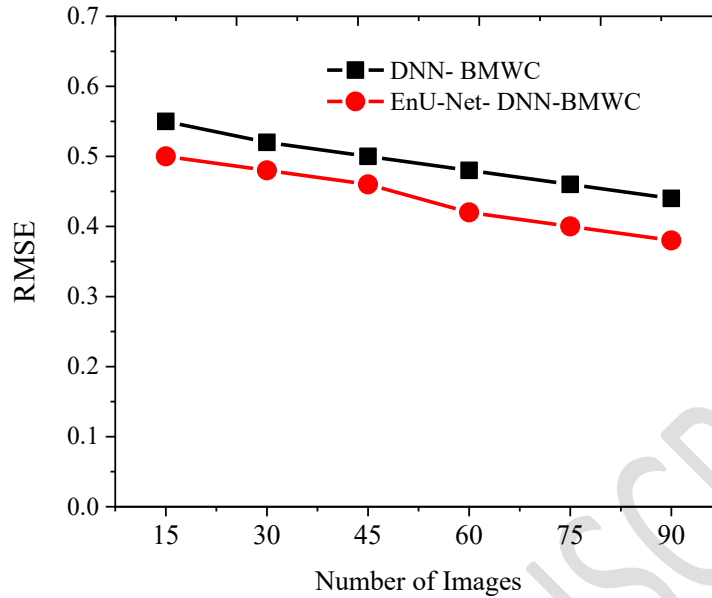
347 0.5, while DNN-BMWC has an RMSE of 0.55. This performance gap widens with each increment

348 in the number of images, with EnU-Net-DNN-BMWC consistently reducing its RMSE by 0.02 to

349 0.07 for each subsequent stage. By the time the dataset reaches 90 images, EnU-Net-DNN-BMWC

350 achieves an RMSE of 0.38, indicating its superior accuracy in predicting values compared to the

351 baseline DNN-BMWC model.



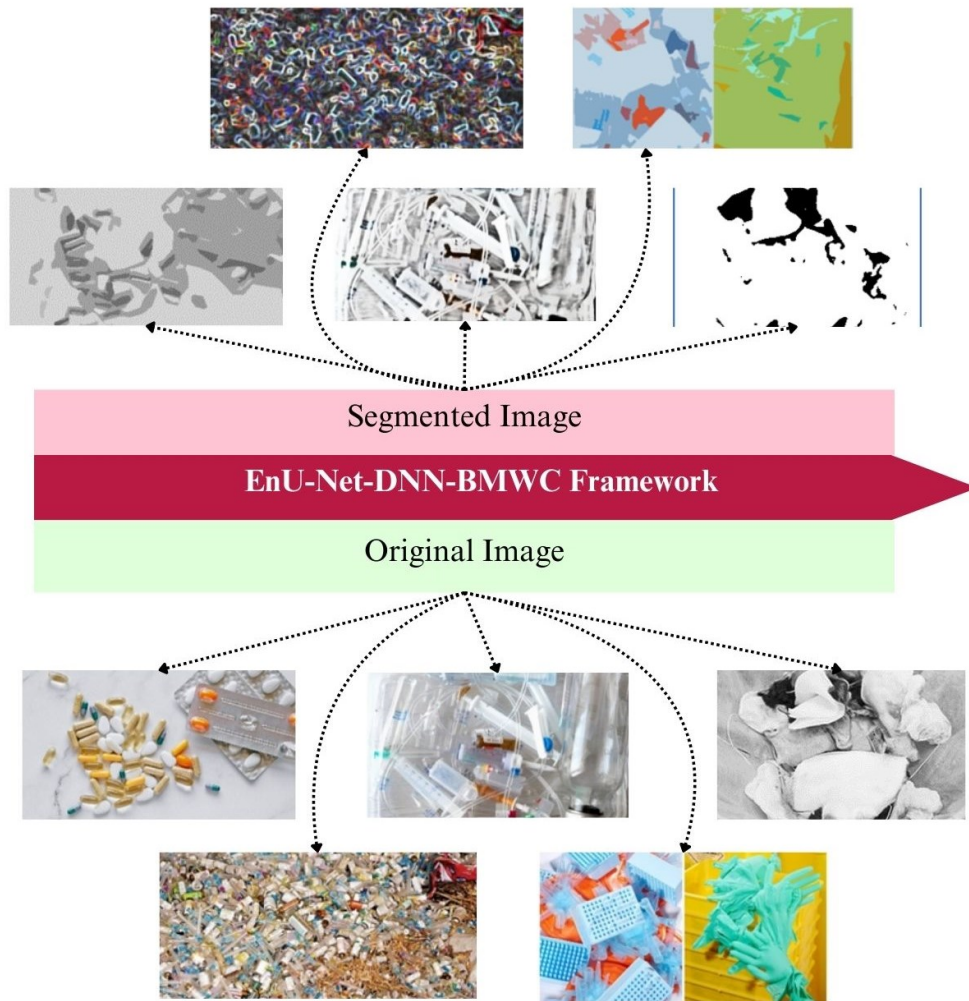
352

353 **Figure 10:** Comparing the Proposed EnU-Net-DNN-BMWC with the RMSE of DNN BMWC

354 EnU-Net-DNN-BMWC framework segmented pictures are shown in Figure 11 together with  
 355 example pairs of original photos. Each pair provides visual evidence of how well the framework  
 356 segments things in the photos. When compared to the segmented photos, which show the exact  
 357 borders and classifications that the EnU-Net-DNN-BMWC model accomplished, the original  
 358 photographs display a range of complexity and richness, from basic to detailed scenarios.

359 This graphic comparison highlights how the framework may improve picture segmentation tasks  
 360 by using its sophisticated architecture, which combines improved feature learning and  
 361 segmentation capabilities to provide accurate and dependable segmentation outputs on a variety of  
 362 image datasets.

363



364

365 **Figure 11:** Original and segmented picture samples for the EnU-Net-DNN-BMWC Framework

366 **4. Discussion**

367 The comparative analysis of the EnU-Net-DNN-BMWC framework against the baseline DNN-  
 368 BMWC model demonstrates significant enhancements across various performance metrics,  
 369 underscoring the effectiveness of the proposed architecture in biomedical waste classification.

370 The consistent improvement in accuracy, precision, recall, F-measure, and reduced error rates  
 371 and RMSE values highlights the robustness of the EnU-Net-DNN-BMWC approach.

372 Starting with a modest dataset, the EnU-Net-DNN-BMWC achieves notable advancements in all  
373 metrics as the number of images increases. This trend indicates that the enhanced segmentation  
374 capabilities of the U-Net architecture effectively feed the DNN, allowing it to leverage more  
375 precise input for classification tasks. For instance, the significant gain in recall, culminating in an  
376 impressive score at larger dataset sizes, illustrates the model's superior ability to identify relevant  
377 instances accurately. Moreover, the lower error rates and RMSE values signify improved  
378 reliability in predictions, crucial for practical applications in biomedical waste management where  
379 misclassifications can have serious consequences.

380 The visual comparisons of segmented images further emphasize the framework's efficacy in  
381 delineating complex features, showcasing the model's ability to handle diverse scenarios and  
382 improve segmentation accuracy. This combination of quantitative and qualitative results positions  
383 the EnU-Net-DNN-BMWC as a formidable tool for automated biomedical waste classification,  
384 promising enhancements in operational efficiency and safety in waste management practices.  
385 Overall, the integration of advanced architectures within this framework offers a significant leap  
386 forward in the field.

## 387 **5. Conclusion**

388 To sum up, the ENU-NET-DNN-BMWC framework in this study represents a significant  
389 advancement in the field of biomedical waste management. Through rigorous experimentation and  
390 analysis, this study has demonstrated notable improvements in both segmentation accuracy and  
391 classification efficiency compared to conventional methods. By leveraging deep neural network  
392 architectures and tailored segmentation techniques, our framework not only enhances the precision  
393 of waste classification but also lays the groundwork for more effective and sustainable healthcare

394 waste management practices. Moving forward, further refinements and integration with emerging  
395 technologies hold promise for extending these benefits to broader healthcare settings, thereby  
396 contributing to safer environments and improved public health outcomes globally. Based on the  
397 comparative analysis across different metrics—accuracy, precision, F-measure, recall, error rate,  
398 and RMSE—between DNN-BMWC and the proposed EnU-Net-DNN-BMWC framework, clear  
399 trends emerge.

400 1. EnU-Net-DNN-BMWC consistently outperforms DNN-BMWC in accuracy across varying  
401 dataset sizes. Starting from 15 images, EnU-Net-DNN-BMWC achieves 82% accuracy compared  
402 to 80% for DNN-BMWC, with a consistent 2% improvement maintained at each subsequent stage.  
403 By the conclusion at 90 images, EnU-Net-DNN-BMWC reaches 92% accuracy, underscoring its  
404 superior performance in image classification tasks.

405 2. The precision analysis reveals EnU-Net-DNN-BMWC's superiority over DNN-BMWC as the  
406 dataset size increases. Beginning at 15 images, EnU-Net-DNN-BMWC achieves a precision of  
407 0.83, surpassing DNN-BMWC's 0.8. This lead widens to 0.93 by the time 90 images are processed,  
408 demonstrating EnU-Net-DNN-BMWC's enhanced precision-oriented capabilities.

409 3. EnU-Net-DNN-BMWC consistently achieves higher F-measure scores than DNN-BMWC  
410 across all dataset sizes. Starting at 15 images with an F-measure of 0.81 compared to DNN-  
411 BMWC's 0.77, the gap increases with each increment. By 90 images, EnU-Net-DNN-BMWC  
412 attains an F-measure of 0.89, showcasing its ability to balance precision and recall effectively.

413 4. EnU-Net-DNN-BMWC consistently outperforms DNN-BMWC in recall scores as the dataset  
414 size expands. Starting at 15 images, EnU-Net-DNN-BMWC achieves a recall of 0.8 versus DNN-  
415 BMWC's 0.75, with the gap widening incrementally. By the conclusion at 90 images, EnU-Net-

416 DNN-BMWC achieves a recall of 0.98, highlighting its superior ability to correctly identify  
417 relevant instances.

418 5. The analysis indicates that EnU-Net-DNN-BMWC maintains lower error rates than DNN-  
419 BMWC across increasing dataset sizes. Starting at 15 images with an error rate of 0.16 compared  
420 to DNN-BMWC's 0.2, EnU-Net-DNN-BMWC consistently reduces its error rate by 0.01 to 0.05  
421 at each subsequent stage. By 90 images, it achieves an error rate of 0.11, showcasing its  
422 effectiveness in minimizing classification errors.

423 6. EnU-Net-DNN-BMWC achieves lower RMSE values than DNN-BMWC as the dataset size  
424 grows. Beginning at 15 images with an RMSE of 0.5 compared to DNN-BMWC's 0.55, EnU-Net-  
425 DNN-BMWC consistently reduces its RMSE by 0.02 to 0.07 at each stage. By 90 images, it  
426 achieves an RMSE of 0.38, demonstrating its superior accuracy in predicting values.

427 Overall, the comprehensive evaluation across these metrics consistently demonstrates the superior  
428 performance of EnU-Net-DNN-BMWC over DNN-BMWC in biomedical waste segmentation and  
429 classification tasks, underscoring its potential for enhancing accuracy, precision, recall, error rates,  
430 and predictive capabilities across varying dataset sizes.

#### 431 **Abbreviation**

432 BMW - Biomedical Waste

433 EnU-Net - Enhanced U-Network

434 EDN - Encoder-Decoder Network

435 CSS - Content-Sensitive

436 Kmch - Kovai Medical Center and Hospital

437 **Competing interests**

438 The authors declare that they have no competing interests.

439 **Consent for publication**

440 Not applicable

441 **Ethics approval and consent to participate**

442 Not applicable

443 **Funding**

444 Not applicable

445 **Availability of data and materials**

446 Not applicable

447 **Authors' contribution**

448 Author A: Led the research design and methodology, developed the EnU-Net architecture, and  
449 conducted the initial experiments. Author B: Implemented the DNN-BMWC framework, carried  
450 out the segmentation and classification tasks, and analyzed the experimental results. Author C:  
451 Managed data collection and preprocessing, assisted in the implementation of the EnU-Net-DNN-  
452 BMWC framework, and provided critical feedback on the manuscript.

453 **Acknowledgment**

454 I acknowledge the omnipotent God for His infinite blessings and wisdom throughout this endeavor.  
455 My sincere thanks go to my remarkable co-workers for their consistent support and teamwork,

456 which played a crucial role in our successes and overcoming obstacles. I also wish to express my  
457 heartfelt appreciation to my family for their unending love and encouragement. Finally, I am truly  
458 thankful to all who assisted in the writing and developing this article."

## 459 **References**

460 Achuthan, A., & Madangopal, V. A. (2016). Bio-medical waste segregation based on hybridization  
461 of self-organizing map clusters with particle swarm optimization. *Int J AdvEngg Tech/Vol.*  
462 *VII/Issue I/Jan.-March*, **500**, 508.

463 al-Sulbi, K., Chaurasia, P. K., Attaallah, A., Agrawal, A., Pandey, D., Verma, V. R., ... & Ansari,  
464 M. T. J. (2023). A fuzzy TOPSIS-based approach for comprehensive evaluation of bio-  
465 medical waste management: advancing sustainability and decision-  
466 making. *Sustainability*, **15(16)**, 12565.

467 Costa, J. D., Patel, H., Braganza, V., & Solanki, H. (2023). Impact of a Crisis on Waste  
468 Management Policy Adherence and Practices-A Narrative Review of Bio-Medical Waste  
469 Management during the Covid-19 Pandemic.

470 Galvan-Alvarez, N., Rojas-Casadiago, D., Kafarov, V., & Romo-Bucheli, D. (2023). Prediction of  
471 Biomedical Waste Generation in Sanitary Emergencies for Urban Regions Using  
472 Multivariate Recurrent Neural Networks. In *Computer Aided Chemical Engineering*, **52**,  
473 1307-1312. Elsevier.

474 Gopi, G., Joshua, S. C., Prabu, K. D., & Janarthanan, M. (2020). BIO MEDICAL WASTE  
475 CLASSIFICATION AND ITS DISPOSING METHODS USING ML. *Indian Journal of*  
476 *Engineering, Science, and Technology*, **14**, 74.

477 Kannadhasan, S., & Nagarajan, R. (2022). Recent trends in bio-medical waste, challenges and  
478 opportunities. *Machine Learning and Deep Learning Techniques for Medical Science*, 97-  
479 108.

480 Kumbhar, M. M., Sethy, P. S., Swain, S., & Kaur, D. (2024). Emerging Technologies for Effective  
481 Disposal and Sustainable Management of Biomedical Waste (BMW) During COVID-19  
482 Pandemic. *Impact of COVID-19 Waste on Environmental Pollution and Its Sustainable  
483 Management: COVID-19 Waste and Its Management*, 171-195.

484 Pavithiran, P., Bhatia, A., Verma, A., Shah, N. R., Pratyush, P., Shanmugarajan, V., & Duraiswamy,  
485 S. (2022). Accumulation of biomedical waste due to COVID-19: Concerns and strategies for  
486 effective treatment to control the pandemic.

487 Sarkar, O., Dey, A., & Malik, T. (2023). Modernized Management of Biomedical Waste Assisted  
488 with Artificial Intelligence. *International Journal of Biomedical and Clinical Analysis*, **3**,  
489 69-86.

490 Sengeni, D., Padmapriya, G., Imambi, S. S., Suganthi, D., Suri, A., & Boopathi, S. (2023).  
491 Biomedical waste handling method using artificial intelligence techniques. In *Handbook of  
492 Research on Safe Disposal Methods of Municipal Solid Wastes for a Sustainable  
493 Environment* (306-323). IGI Global.

494 Shang, D., Zhang, F., Yuan, D., Hong, L., Zheng, H., & Yang, F. (2024). Deep Learning-Based  
495 Forest Fire Risk Research on Monitoring and Early Warning Algorithms. *Fire*, **7**, 151.

496 Subramanian, A. K., Thayalan, D., Edwards, A. I., Almalki, A., & Venugopal, A. (2021).  
497 Biomedical waste management in dental practice and its significant environmental impact:  
498 A perspective. *Environmental Technology & Innovation*, **24**, 101807.

499 Wawale, S. G., Shabaz, M., Mehbodniya, A., Soni, M., Deb, N., Elashiri, M. A., & Naved, M.  
500 (2022). Biomedical Waste Management Using IoT Tracked and Fuzzy Classified Integrated  
501 Technique. *Human-centric Computing and Information Sciences*, **12**, 32.

502 Zulqarnain, R. M., Naveed, H., Askar, S., Deveci, M., Siddique, I., & Castillo, O. (2024).  
503 Assessment of bio-medical waste disposal techniques using interval-valued q-rung orthopair  
504 fuzzy soft set based EDAS method. *Artificial Intelligence Review*, **57**, 210.

ACCEPTED MANUSCRIPT